6-2013

A Mathematical Model of Renal Cell Carcinoma

Taylor M. Broome
College of William and Mary

A Mathematical Model of Renal Cell Carcinoma

A thesis submitted in partial fulfillment of the requirement
for the degree of Bachelor of Science in Chemistry from
The College of William and Mary

by

Taylor Michelle Broome

Accepted for _____

_____
Randolph Coleman, Director

_____
Christopher Abelt

_____
Mark Forsyth

Williamsburg, VA
April 24, 2013

Abstract

Renal cell carcinoma (RCC) is an incredibly deadly type of kidney cancer. This paper catalogs the creation of a mathematical model of RCC. The model focuses on transcriptional regulation via hypoxia-inducing factor (HIF), nuclear factor kappa B (NFκB), Myc-Max, p53, and the mammalian target of rapamycin (mTOR) pathway ; cell metabolism and cell cycle regulation are also analyzed. A model of a healthy renal cell and a renal cell carcinoma were created. When the two models were compared mathematically, it was found that the disease state seemed to mimic the behavior of the cancer in vivo. Because of its perceived accuracy, the disease model was treated with two current RCC chemotherapeutics: sunitinib and everolimus. The treatments proved moderately effective, so a cocktail treatment of the drugs was also modeled. Despite the success of the cocktail treatment in the mathematical model, in actual drug trials the cocktail treatment proved toxic. This leads to the conclusion that more research needs to be conducted, perhaps on different areas of the disease that could potentially be less toxic and more effective in treating RCC.

Acknowledgements

First, I would like to thank Dr. Randolph Coleman for being my mentor over the past four years. Words cannot express my gratitude to Dr. Coleman. I have reached heights that I never thought myself capable of reaching, and I truly owe it to his support over the years. I would also like to thank Dr. Mark Forsyth and Dr. Christopher Abelt for graciously agreeing to be on my committee. Additionally, I would like to thank my donors Mr.

Stuart Miller and Mrs. Margaret Focarino. Without their generous financial support, none of this would have been possible.

I would like to thank my family and friends for supporting me throughout this endeavor. I would like to give a special thank you the Coleman Group, particularly my fellow Avengers: Amy Roach, Emily Rose Bainwol, Pete Calcagni, Alex Chartrain, and Kenneth Qiu. They were always there to make me smile and distract me from my work when things got rough.

Finally, I would like to thank Alex Chinn for performing the thankless task of adding whimsy to my life. If I have, in fact, remained sane throughout this process, it is due entirely to him.

1. Introduction

Renal cell carcinoma (RCC) is the most common type of kidney cancer and accounts for 3% of all adult cancers (Morais, 2011). Symptoms of the cancer typically include abdominal pain, blood in the urine, and system paraneoplastic syndromes associated with excess proteins secreted in the disease (Rini, 2009). Though these symptoms present late in RCC, the cancer is often caught early during radiological exams for alternative reasons. Despite its often early detection, the mortality rate with RCC remains high with patients surviving four months on average and only 10% of patients living past one year (Morais, 2011). RCC is actually a group of cancers containing both sporadic (non-inherited) and familial types. The most common type of RCC is the sporadic clear cell RCC (ccRCC), which accounts for 75% of cases (Brugarolas, 2009). ccRCC is so-named

due to the high lipid content of the cytoplasm that gives the tissue a clear appearance during staining (Rini, 2009).

Treating RCC is exceptionally difficult due the wide variety of presentations of RCC. The most common treatment is either partial or total removal of the kidney, the degree to which depends on whether or not the tumor is localized (Morais, 2011). Radiation therapy is another option; however, the kidney is more susceptible to radiation damage than other locations. Immunotherapy with interferon-alpha (IFN-α) or interleukin-2 (IL-2) is effective in a small subset of patients, but the treatment itself is associated with nephrotoxicity. Chemotherapy is also largely ineffective against RCC. In a 2000 analysis conducted by Motzer and Russo, 51 phase II trials of 33 chemotherapeutic agents were analyzed; none of the agents were found particularly effective against RCC (Motzer, 2000). The degree to which current treatments are inadequate in the fight against RCC has taken the focus in RCC from traditional cancer therapies to more new chemotherapeutics with novel biological mechanisms.

One way to study these novel biological mechanisms is that of biochemical systems theory (BST). BST was created by Savageau in 1969 and later expanded upon by Voit in 2000 (Sass, 2009). The purpose of BST is to provide a mathematical framework on which a biochemical system can be analyzed, even when little experimental information is known about the system. BST can be used to produce a qualitative model of a biological system in order to ascertain information about potential therapies. In this study, BST was used to create a baseline, disease, and treatment state for a mathematical model of RCC. This model focuses on three main areas within RCC: transcriptional regulation, cell metabolism, and cell cycle regulation. Though these areas are broad, they are by no

means mutually exclusive. The key players in transcriptional regulation within the model are NFκB, p53, hypoxia-inducible factor (HIF), c-myc, and the mammalian target of rapamycin (mTOR) pathway. Each of these proteins play a role in either sending the renal cell closer or farther from a tumorigenic state. Cell metabolism within the model focuses mainly on the Warburg effect, the metabolic phenotype shift observed in tumor cells whereby ATP generation via oxidative phosphorylation shifts to ATP generation through glycolysis even under normal oxygen conditions (Cairns, 2011). The cell cycle regulation facet of the model deals with the cellular battle between cell cycle progression and programmed cell death and the players in between.

2. Methods

This section details the methods by which a mathematical model of renal cell carcinoma was created and analyzed. First, a visual model of the biochemical interactions within a renal cell was created using Cell Designer (Kitano, 2005). Then, the visual model was converted into a system of differential equations, initial values, and system equations via a program called power law analysis and simulation (PLAS) (http://www.dqb.fc.ul.pt/docentes/aferreira/plas.html, link no longer available). Finally, the PLAS output was analyzed using Microsoft Excel in order to visualize the data.

2.1. Modeled Cellular Pathways

2.1.1. pVHL

The von Hippel-Lindau (VHL) gene acts a tumor suppressor in RCC. Recent studies have reported that the VHL gene is inactivated by DNA methylation in as many as 90% of clear cell RCC cases (Herman, 1994). This high correlation between ccRCC and the loss of the VHL gene makes the gene and the subsequent protein, pVHL, molecules of interest in the disease. pVHL is involved in the regulation of the cellular environment by responding to changes in oxygen levels (Brugarolas, 2009). When oxygen levels are high, pVHL acts as an E3 ligase and ubiquitinates hypoxia-inducible factor-alpha (HIF-α) (Model 1). When HIF-α is not degraded, it complexes with HIF-β to form HIF, a transcription factor involved in a multitude of cellular processes (Hervouet, 2007). HIF activates the transcription of vascular endothelial growth factor (VEGF) and platelet-derived growth factor beta (PDGF-β), both of which lead to angiogenesis, which leads to the spread of cancer. HIF also affects glucose metabolism by activating the transcription of glucose transporter-1 (Glut-1), lactate dehydrogenase (LDH), and phosphoinositide-dependent kinase-1 (PDK-1). Activation of these proteins leads to an overall increase in glycolysis, but an overall decrease in the tri-carboxylic acid cycle and oxidative phosphorylation. HIF also acts as a transcription factor for the production of regulated in development and DNA damage responses 1 (REDD1) and transforming growth factor beta (TGF-β) (Abraham, 2012; Hervouet, 2007). REDD1 acts as an inhibitor of the mammalian target of rapamycin (mTORC) pathway and TGF-β acts to inhibit the cell cycle by activating the transcription cyclin-dependent kinase inhibitors (CKIs) p27 and p15. Additionally, pVHL itself is said to somehow inhibit the production of NFκB, but the exact mechanism is unknown (Morais, 2011).

Model 1. Role of pVHL and HIF in RCC.

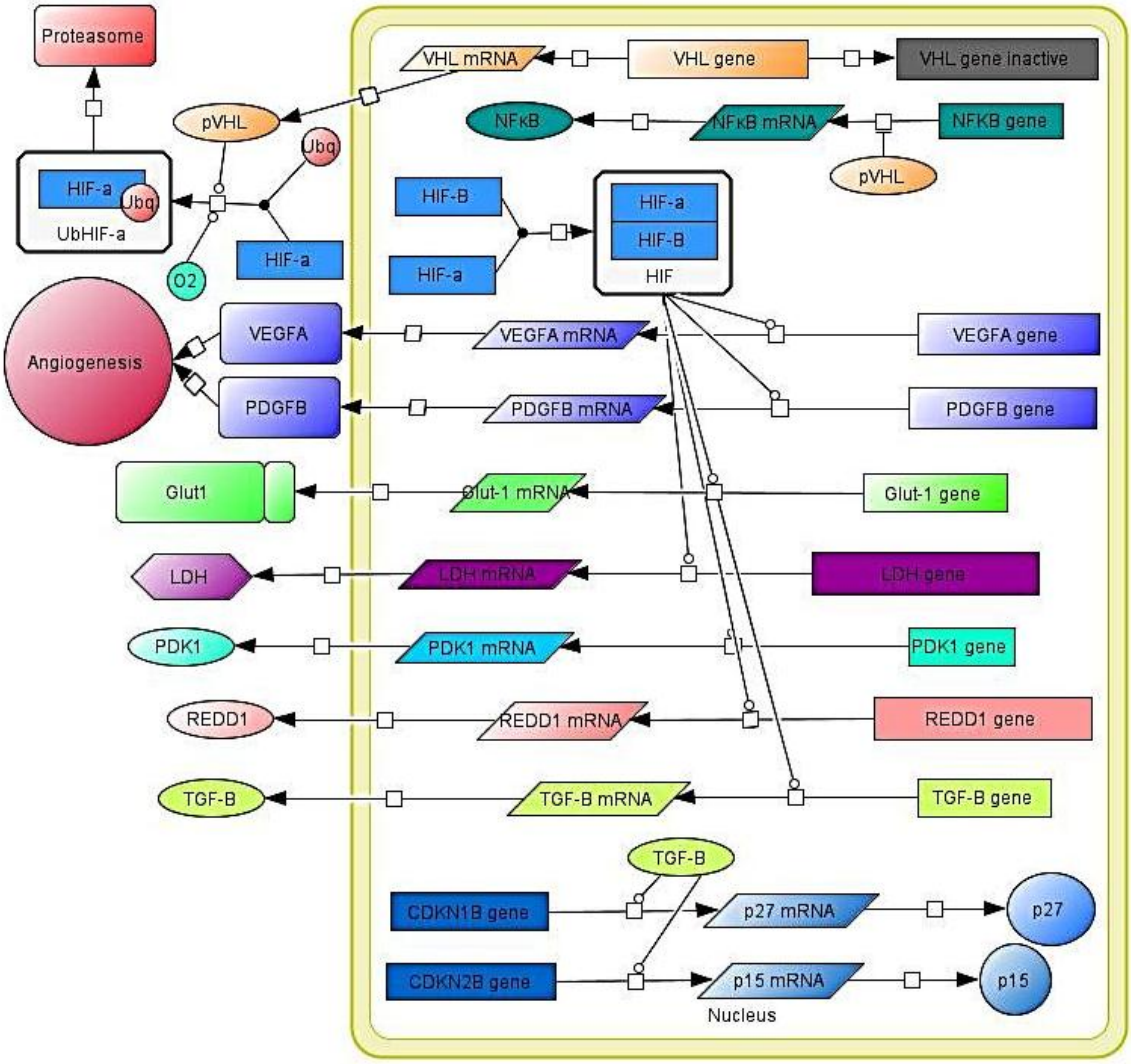

2.1.2. p53

The tumor suppressor p53 is one of the most studied molecules in science due to its pivotal role in cell cycle regulation and cancer. It is perhaps best known for its role in sensing DNA damage and promoting apoptosis, but it is now known to be heavily involved in cell metabolism (Cairns, 2011). p53 becomes activated when ataxia telangiectasia mutated (ATM) kinase and ATM and Rad3-related (ATR) kinase are

activated by DNA damage (Model 2) (Noon, 2010). The transcription of p53 is also inhibited by NFκB (Morais, 2011). Activated p53 acts by promoting transcription of many proteins involved in the cell cycle and in metabolism (Noon, 2010). p53 activates the expression of hexokinase IV (HKIV), which converts glucose to glucose-6-phosphate in glycolysis (Cairns, 2011). However, p53 can also have a negative effect on glycolysis by upregulating the expression of TP53-induced glycolysis and apoptosis regulator (TIGAR), which decreases the level of fructose-2,6,-bisphosphate, a glycolytic activator. Additionally, p53 promotes oxidative phosphorylation by activating the transcription of SCO2, a protein involved in the electron transport chain. Another protein that is upregulated by p53 is glutaminase 2 (GLS2), which converts glutamine into glutamate in the formation of glutathione. In addition to its role in metabolism, p53 also plays a huge role in cell cycle regulation via upregulating the production of Bax and p21 (Vermeulen, 2003). Bax is a pro-apoptotic protein that complexes with Bak to form the mitochondrial apoptosis-induced channel (MAC), which release apoptotic factors from the mitochondria (Khan, 2010). When the MAC is opened, cytochrome C, apoptosis-inducing factor (AIF), and endonuclease G exit the mitochondria and cause cellular damage leading to apoptosis. p21 is a CKI that results in the inhibition of CDK and cell cycle arrest. p53 also upregulates the production of murine double minute 2 (MDM2), a negative regulator of p53 (Noon, 2010). MDM2 binds to p53 and acts as an E3 ligase to ubiquitinate p53 for destruction in the proteasome. Since p53 promotes MDM2 production and MDM2 production leads to p53 degradation, these species form a negative-feedback loop and as such the concentrations of these two proteins are often linked within a cell. MDM2 can itself be inactivated when it is bound to tumor suppressor p19 (Vermeulen, 2003). In

addition, p53 activates the transcription of phosphate and tensin homolog (PTEN), which acts a tumor suppressor and prevents activation of the mTOR pathway (Cairns, 2011).

Model 2. Role of p53 in RCC.

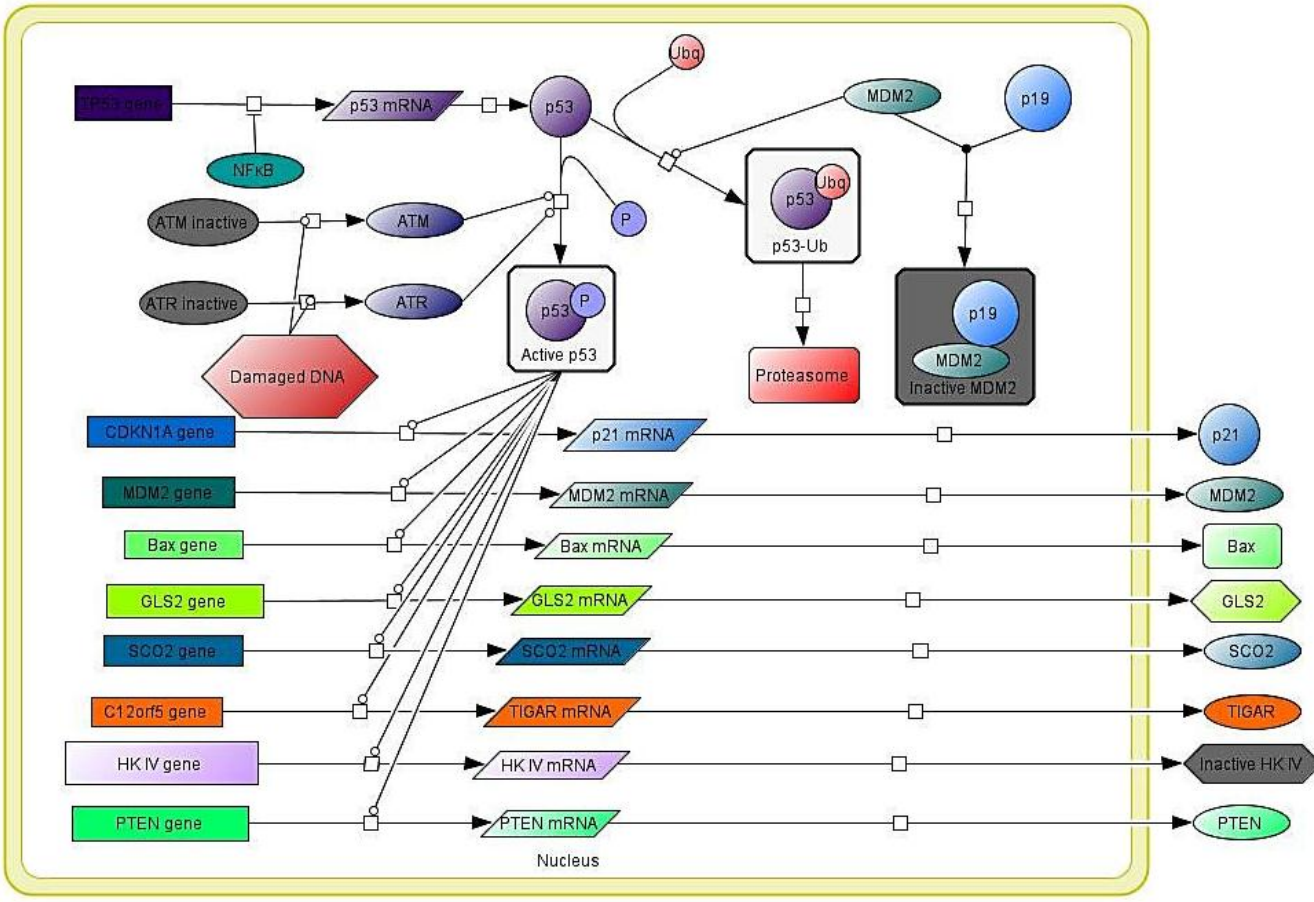

2.1.3. NFκB

NFκB seems to function primarily as a survival signal for oncogenic cells in renal cell carcinoma (Morais, 2011). NFκB activates the transcription of cyclins A, B, D, and E, angiogenic growth factor VEGFA, MRP, P-gp, and cFLIP (Model 3). Cyclins A, B, D, and E all promote cell cycle progression and overactivation of these proteins can lead to cancer. MRP and P-gp are both membrane transport proteins that export drugs across the cell membrane using ATP. In RCC, these proteins are upregulated in order to keep anti-cancer drug concentrations low in the cell; this contributes to the multidrug resistance

observed in RCC. Cellular FLICE inhibitory protein (cFLIP) is an anti-apoptotic protein that inhibits the activation of caspase 8; its activation contributes to the anti-apoptotic potential of NFκB. NFκB itself can be activated when it is released from the IKK complex. This occurs during death receptor signal transduction via tumor necrosis factor (TNF) complex I, which causes NFκB to be released from the IKK complex (Micheau, 2003). NFκB can also be released from the IKK complex by the kinase AKT.

Model 3. Role of NFκB in RCC.

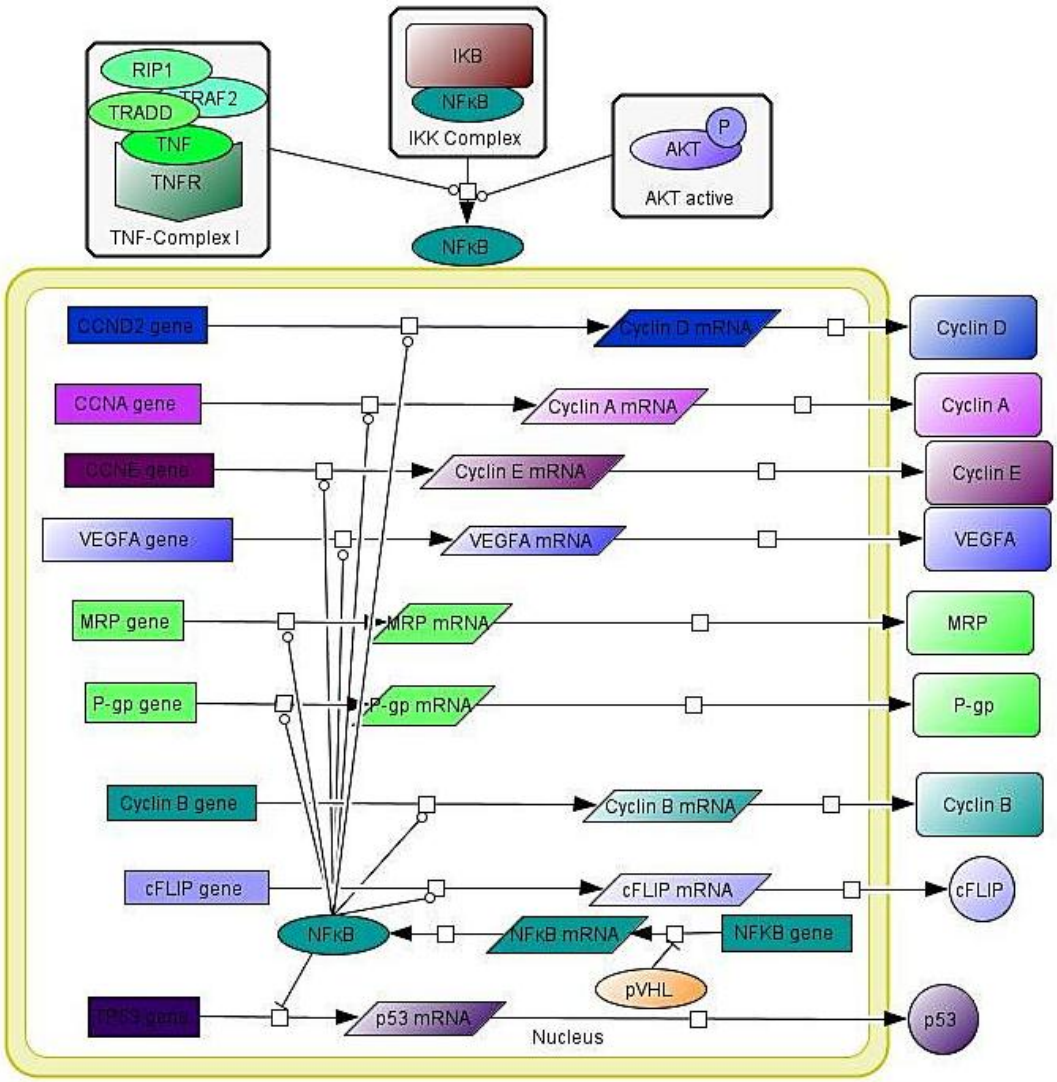

2.1.4. Myc-Max

Myc plays an important role in normal cell growth and proliferation; in fact, an estimated 10-15% of genes are regulated by Myc (Larsson, 2010). Deregulation of Myc can result in not only tumorigenesis, but also the triggering of intrinsic cellular tumor suppression mechanisms. Myc itself is only able to act as a transcription factor when bound to the constitutively expressed Max (Lutz, 2002). In RCC, Myc-Max has a profound effect on cell metabolism and cell cycle regulation. Myc-Max promotes cell cycle progression by upregulating the transcription of cyclin D, CDK4, DNA-binding protein inhibitor ID-2 (ID2), cyclin-dependent kinases regulatory subunit 2 (Cks2), and cullin 1 (Cul-1) (Model 4). CDK4 and cyclin D form a complex that promotes cell cycle progression directly and indirectly via the sequestration and subsequent phosphorylation of tumor suppressor p27. Once p27 has been phosphorylated at threonine 187 by the CDK4/cyclin D complex, an E3 ligase composed of Cul-1, Cks2, and another protein S-phase kinase-associated protein 2 (Skp2) can recognize and ubiquitinate p27. ID2 binds to and sequesters retinoblastoma (pRb) protein to prevent it from binding to E2F. E2F in its unbound form is free to activate the transcription of genes necessary for cell cycle progression. Myc also plays a role in cell glucose metabolism and anti-oxidant production. Myc has been found to promote the preferential expression of the lower affinity pyruvate kinase M2 (PKM2) over the higher affinity PKM1 (Cairns, 2011). Pyruvate kinase is responsible for the conversion of phosphoenolpyruvate to pyruvate, an essential step in glycolysis. So the stalling action by PKM2 allows the glycolytic precursors to be shunted to other biosynthetic pathways, a phenomenon often observed in tumor cells via the Warburg effect. Myc-Max also influences the production of the anti-oxidant glutathione (GSH).

First, Myc-Max indirectly increases amounts of GLS1, an enzyme that controls the first step in GSH synthesis, by degrading microRNA-23A and microRNA-23B, which would otherwise inhibit GLS1. Second, Myc-Max upregulates the production of glutamine transporters SLC5A1 and SLC7A1, which import glutamine, increasing the amount of glutamine available for GSH synthesis.

Model 4. Role of Myc-Max in RCC.

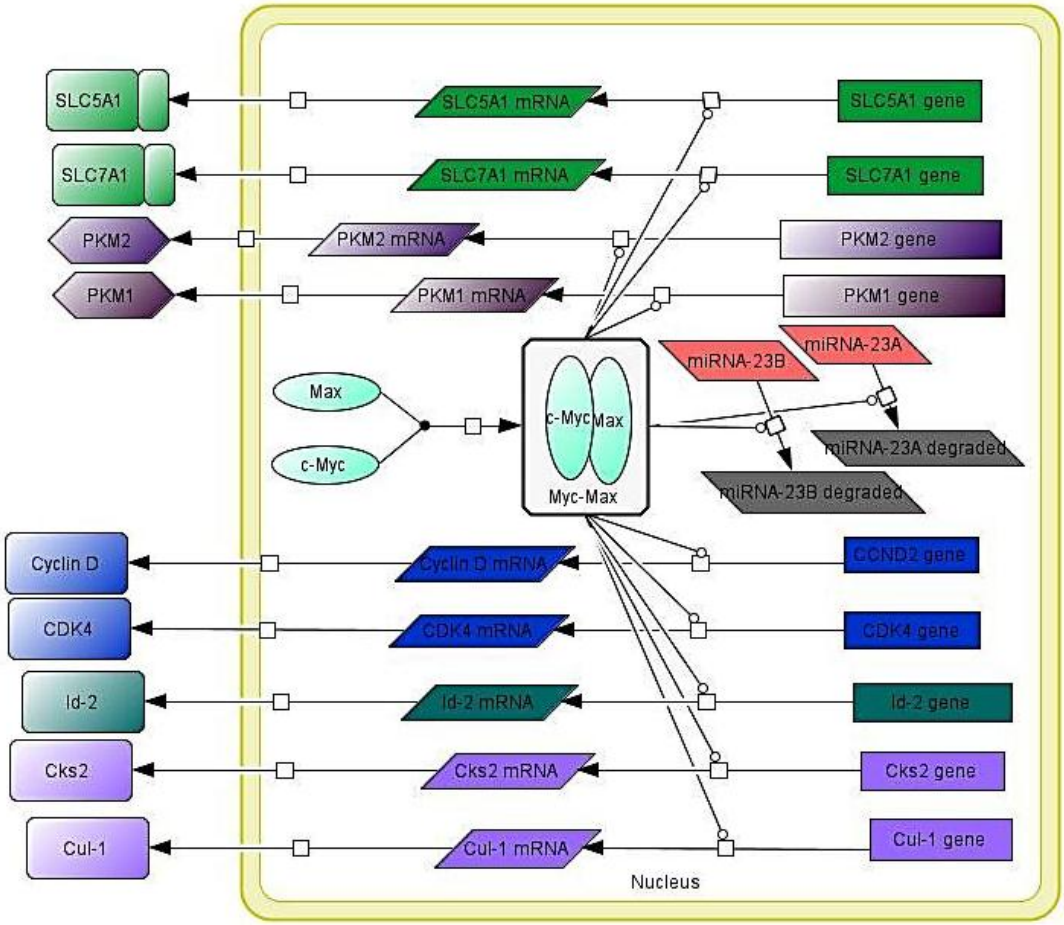

2.1.5. mTOR Pathway

The target of rapamycin (TOR) proteins are members of the phosphoinositide 3-kinase-related kinase (PIKK) family, whose members are tasked with transmitting signals related to cell growth and proliferation (Abraham, 2007). Of the mTOR pathway, the model

focuses on the activation of mammalian TOR complex I (mTORCI) and protein kinase B (AKT) (Model 5). The activation of AKT begins with the binding of the pleckstrin homology domain (PH) of AKT to phosphatidylinositol trisphosphate (PIP3); this releases the inhibitory function of the PH domain and AKT is now free to be activated (Hara, 2005). PTEN can inhibit this process by dephosphorylating and inactivating PIP3 so that it cannot bind to AKT. If the PH domain is uninhibited, AKT can be activated by mTORCII, phosphoinositide-dependent kinase 1 (PDK1), or phosphoinositide 3-kinase (P13K) (Abraham, 2007). One consequence of AKT activation is the inactivation of the pro-apoptotic protein Bad; deregulation of this process can lead to an oncogenic phenotype (Hara, 2005). Activated AKT also becomes involved in the activation of mTORCI by phosphorylating tuberous sclerosis 2 (TSC2), which activates mTORCI through an unknown mechanism (Abraham, 2007). When TSC2 is unphosphorylated, it binds to TSC1 via the influence of REDD1 and Amp-activated protein kinase (AMPK); AMPK serves as a cellular indicator of energy supply because it is activated by changes in the AMP/ATP ratio as well as the liver kinase B 1 (LKB1) protein. The TSC1/2 complex activates the conversion of Rheb-GTP to Rheb-GDP; Rheb-GTP normally activates mTORCI, so its hydrolysis has an inhibitory effect on mTORCI. Once mTORCI is activated, it activates 4E-BP1 and S6 kinase 1 (S6K1), two proteins involved in translational machinery; this has the effect of increasing the translation of HIF.

Model 5. Role of mTOR pathway in RCC.

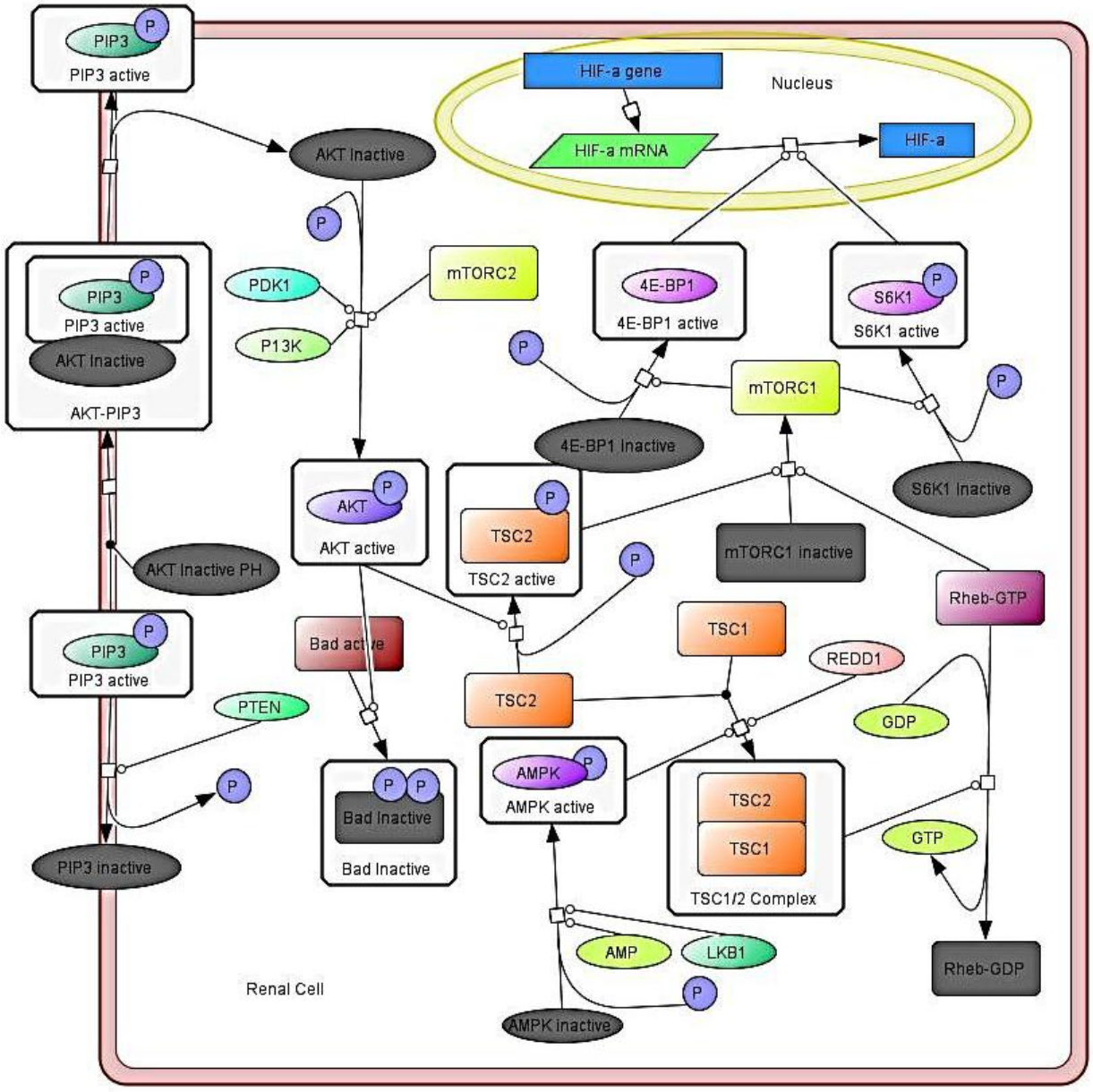

2.1.6. Warburg Effect

Tumors exhibit an anaerobic phenotype of abnormally high glycolysis and low oxidative phosphorylation even in the presence of oxygen (Hamanaka, 2012). This phenomenon, called the Warburg effect is attributed to several reason. First, glycolysis generates ATP

at a faster rate than oxidative phosphorylation, which is useful in proliferating tumor cells. Second, glycolytic intermediates can be shunted into other biosynthetic pathways such as the pentose phosphate pathways, so higher levels of glycolysis contribute to higher levels of glycolytic intermediates. Several proteins are attributed to the shift from ATP production by oxidative phosphorylation to ATP production by glycolysis (Model 6). Glut1 is overexpressed in RCC due to upregulation by HIF, which leads to higher amounts of intracellular glucose available for glycolysis. Hexokinase (HK) converts glucose to glucose-6-phosphate to begin the process of glycolysis (Mathupala, 2006). Normal cells utilize HK IV, but tumor cell often express the higher affinity HK II; this switch increases the amount of glucose being shunted through glycolysis. Phosphofructokinase (PFK-1) is a key regulator of glycolysis by converting fructose-6-phosphate to fructose-2,6-bisphosphate; it is itself inhibited by high levels of ATP and activated by fructose-2,6-bisphosphate (Hamanaka, 2012). Fructose-6-phosphate is also converted into fructose-2,6-bisphosphate, which causes it to self-regulate. This reaction is catalyzed by AKT and inhibited by TIGAR, a protein activated by p53. In addition to promoting glycolysis via fructose-2,6-bisphosphate, AKT also promotes glycolysis by activating HK. Pyruvate kinase (PK), which is activated by Myc-Max, also plays a role in cell metabolism by switching from the PKM1 isoform to the PKM2 isoform. High levels of glycolysis are also maintained by overexpression of LDH, which is activated by HIF. PDK1, an HIF target, binds to and inactivates PDH, the enzyme responsible for the conversion of pyruvate to acetyl coA; this results in decreased oxidative phosphorylation (Hervouet, 2007). SCO2 is stimulated by p53 and attempts to rectify the increased glycolysis by promoting oxidative phosphorylation.

Model 6. The Warburg effect in RCC.

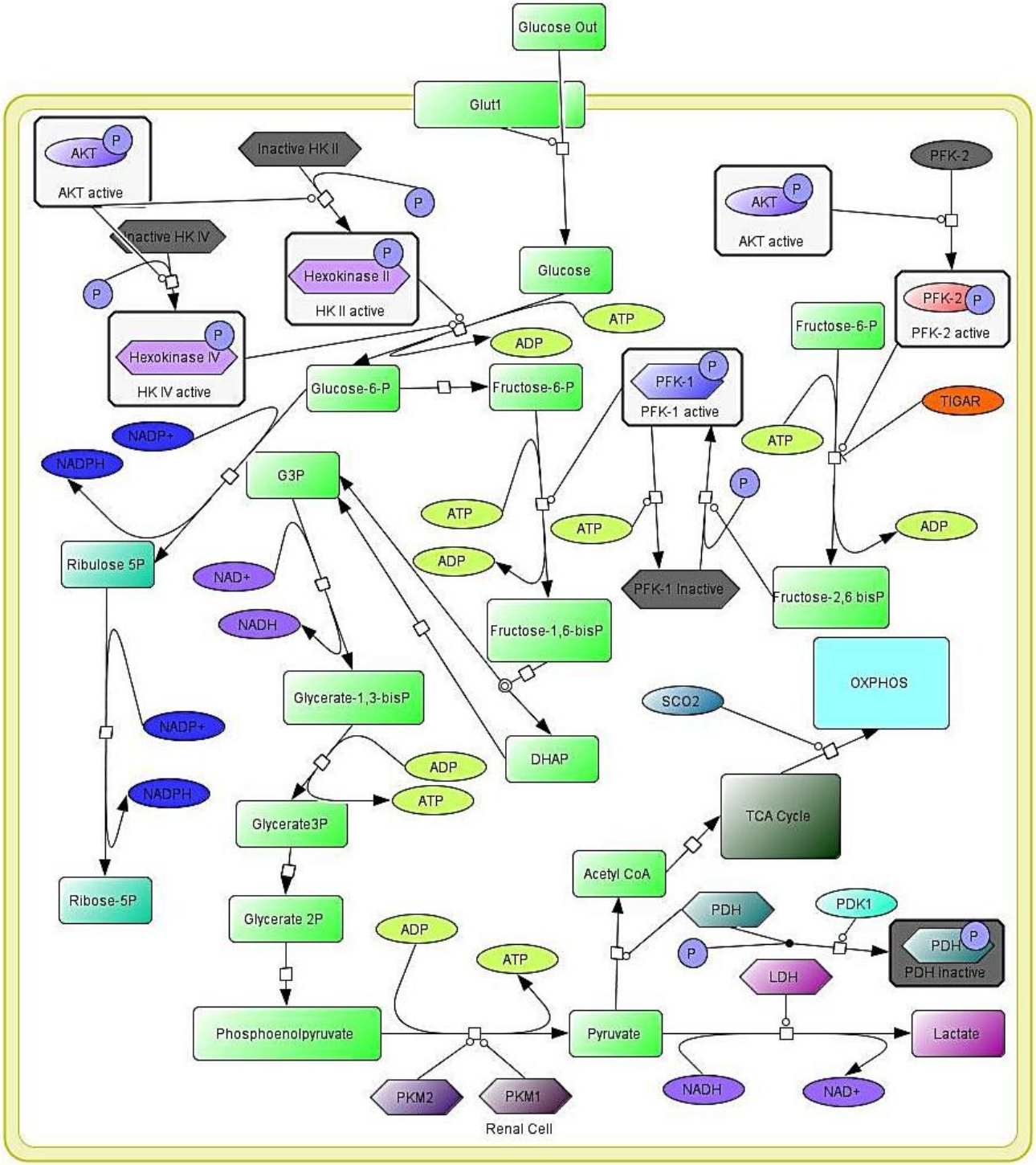

2.2. PLAS

Power law analysis and simulation (PLAS) is a program that uses a system of mathematical equations in order to project concentrations of biochemical species over time. In order to do this, each species and reaction in the model of RCC had to be converted into a mathematical variable and equation, respectively.

2.2.1. Initial Values

The first step of converting the physical model in Cell Designer to a mathematical model in PLAS is to assign each species within the model an X-value. Once all the species are assigned a value, the values are sorted by whether or not the species is a dependent or independent variable. Then, the X- values are assigned initial concentrations in order to more accurately portray a renal cell. For example, glucose was assigned to X9 and set at the initial concentration of 10. The value of 10 is simply our assessment of the relative presence of glucose compared to other cellular species.

2.2.2. Flux Equations

After the initial values are assigned, each reaction in the model is assigned a J-value. Each J-value is associated with a flux equation with a rate constant, k. The X-values for the reactants in the reaction are also incorporated into the flux equation (the X-values for the products will be incorporated into the system equations). For example, the flux equation for the conversion of glucose-6-phosphate to fructose-6-phosphate is J6 = k6 X9^g69, where X9 represents glucose-6-phosphate and k6 and g69 are rate-determining

constants (Model 7). More complicated reactions in the model have other molecules promoting or inhibiting the reaction. This is shown by deriving the k value and multiplying it by the rate constant p for promotion or i for inhibition. For example, fructose-6-phosphate is phosphorylated by PFK-1 into fructose-1,6-bisphosphate (J7). The catalysis by PFK-1 is coded as k7' = 0.001*(p726 X26), where X26 is PFK-1 (Model 7). The k and k' values vary based on the relative rates of the reaction.

Model 7. Flux equations for J6 and J7.

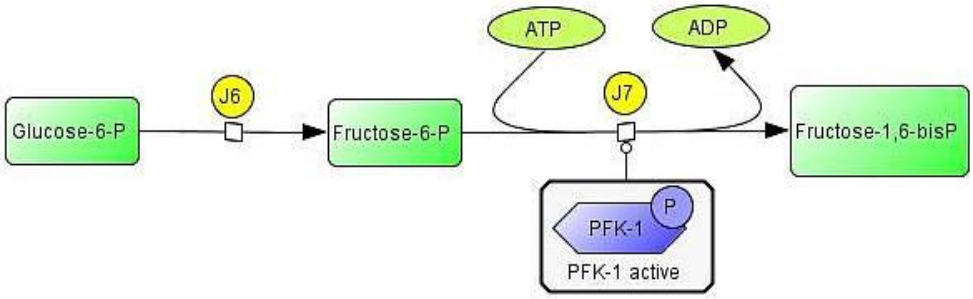

2.2.3. System Equations

The system equations are used to tie the mathematical model together and express the interaction between different species in the model. Each dependent variable is given a system equation called the X-value prime; for example, the system equation for X2 Glut1 is X2'. Then the system equation is set equal to the J-values that feed into or away from that species. For instance, ribulose-5-phosphate (X11) is created by J5 and used up by J14, so the system equation is X11' = J5 - J14 (Model 8).

Model 8. System equation for ribulose-5-phosphate.

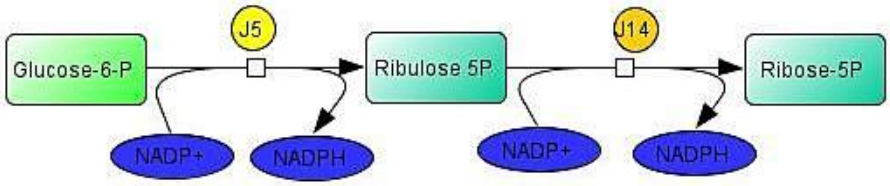

2.3. Excel

PLAS can express reaction rates and concentrations of biochemical species over time as a table of values. Microsoft Excel is used for comparing these tables for the baseline versus disease state and the disease state versus treatment state. Once a percent change between the two graphs is calculated, graphs of species of interest can be generated and used to visualize the information.

3. Results

3.1. Disease State

The tables in this section detail the results of disease state of RCC. The disease model for pVHL (Figure 1) was made by decreasing the rate of pVHL transcription and increasing the rate of pVHL inactivation. Additionally, HIF was increased by increasing the reaction rate of the formation of HIF.

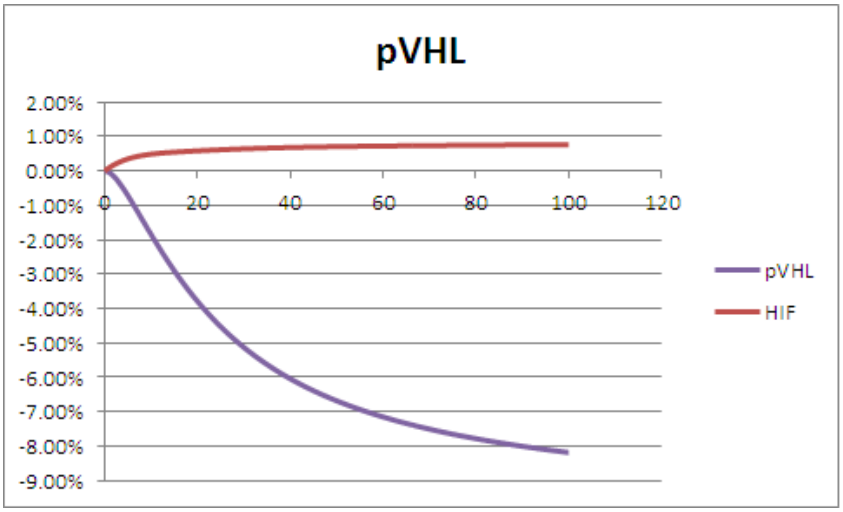

Figure 1. Levels of pVHL and HIF in the disease state model of RCC.

The increase in HIF resulted in an increase in the production of ribose-5-phosphate and lactate, as well as an increase in acetyl coA and oxidative phosphorylation (Figure 2); these findings are consistent with the Warburg effect. Also, the isoforms of hexokinase and pyruvate kinase were switched in the disease state as observed in the literature. Additionally, the equations for the conversion of pyruvate into lactate and the inactivation of PDH were also increased in the disease state, to further simulate the Warburg effect.

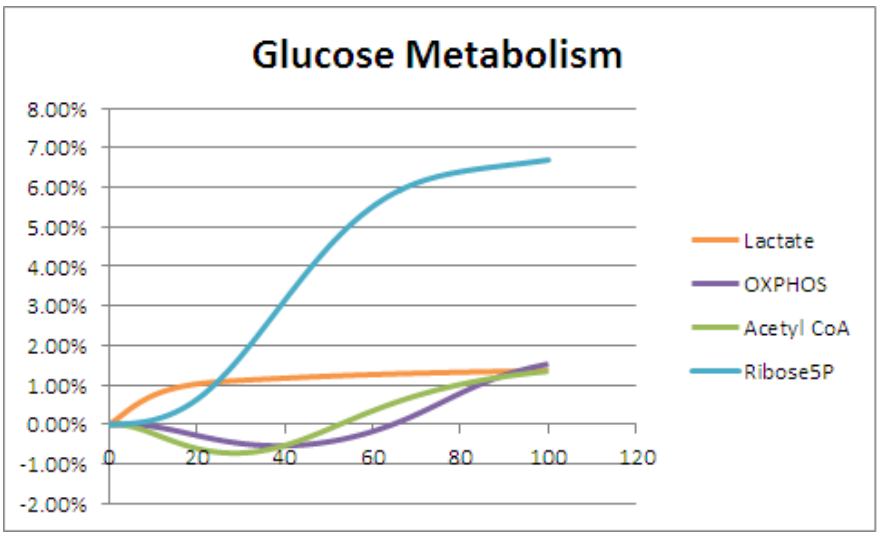

Figure 2. Effects of disease state of RCC on glucose metabolism.

Levels of Myc-Max were increased in the disease state by increasing the rate of formation of Myc-Max (Figure 3). NFκB concentration, however, was increased indirectly by releasing the inhibition that pVHL normally has over NFκB.

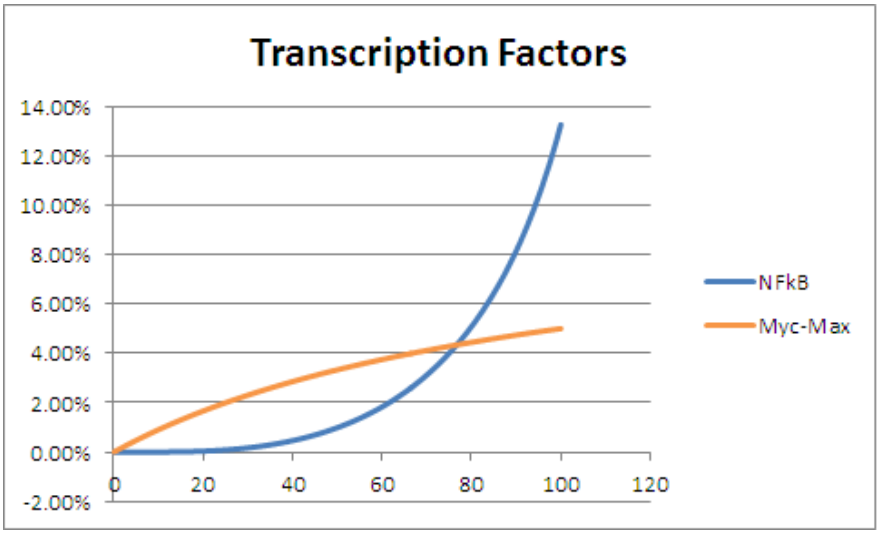

Figure 3. Concentrations of transcription factors in the disease state.

The concentration of p53 was increased by increasing the rate constant for the transcription and translation of p53 (Figure 4). This change also increased the levels of MDM2, which is under the transcriptional control of p53. MDM2 also serves as a negative-feedback regulator of p53.

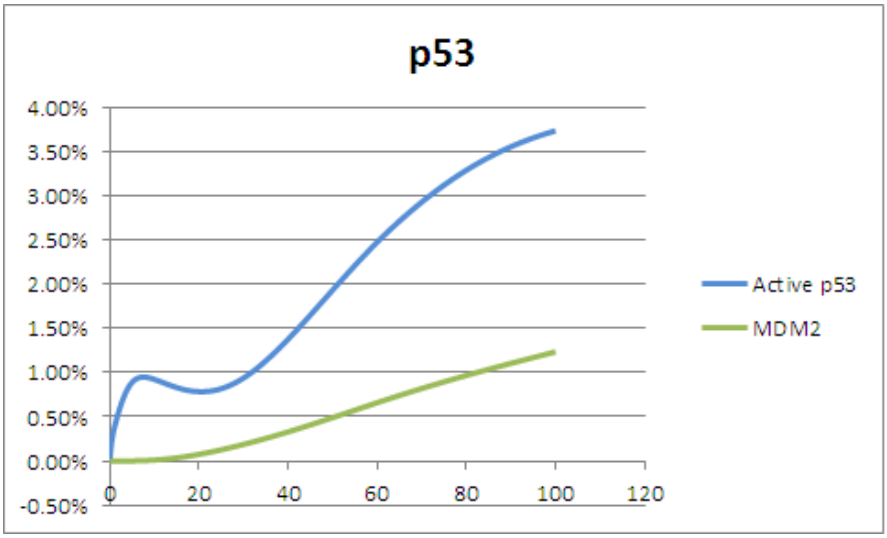

Figure 4. Levels of p53 and MDM2 in the disease state model of RCC.

The concentrations of activated AKT and mTORCI were increased by downstream effects of some of the other changes in the disease state model (Figure 5 and 6). For example, concentrations of PTEN, an inhibitor of the mTOR pathway were reduced in the disease state, and this change could account for some of the increase observed.

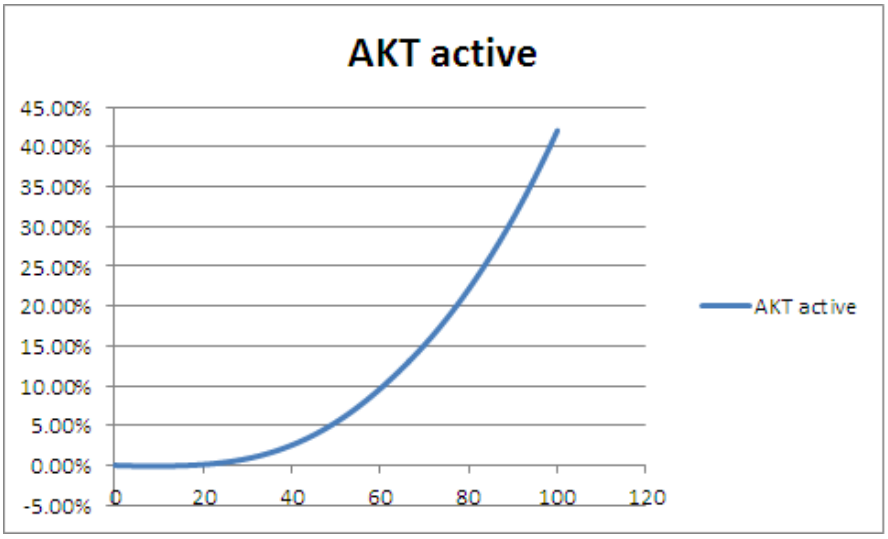

Figure 5.Concentration of activated AKT protein in disease state model of RCC.

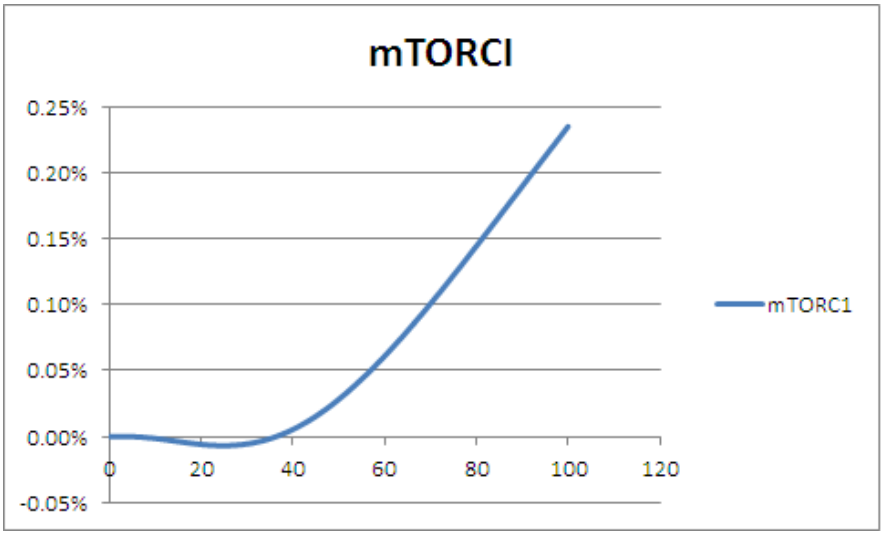

Figure 6. Concentration of mTORCI in disease state model of RCC.

The overall effect of the disease state can be measured in three markers of cancer: apoptosis, angiogenesis, and mitosis (Figure 7). The rate of apoptosis is decreased in the disease state, as would be expected in a tumorigenic state. This decrease is due to the increase in MAC formation due to an increase in the activity of the pro-apoptotic protein Bcl-2 and to the decrease in apopotosome formation due to pro-apoptotic protein Bcl-XL. Angiogenesis is promoted in the disease state by an increase in NFκB and HIF. The disease state promotes mitosis in numerous downstream ways such as the activation of cyclins and CDKs by transcription factors.

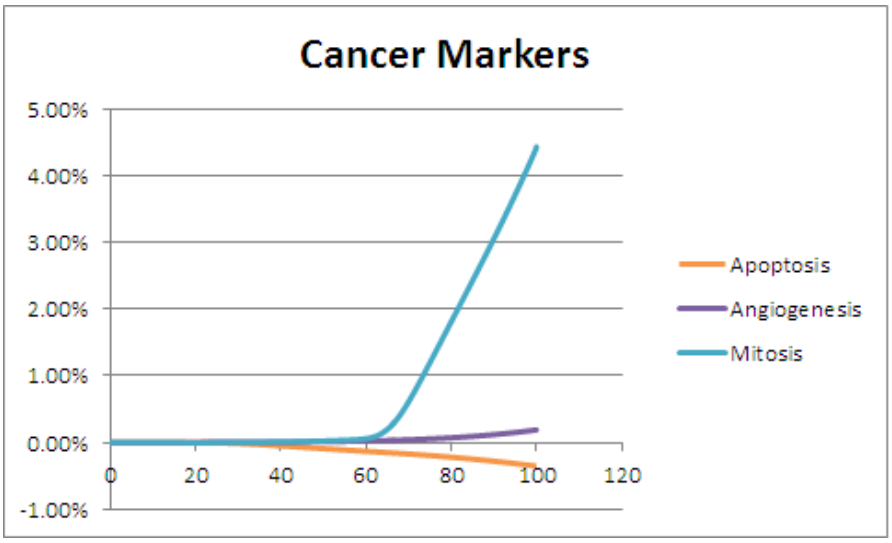

Figure 7. Cancer markers of interest in the disease state model of RCC.

3.2. Treatment State

3.2.1. Angiogenesis Inhibitor

This treatment state mimics the effects of the drugs sunitinib, a drug that inhibits receptor tyrosine kinases such as the VEGF receptor and PDGF-β receptor; this has the effect of reducing the angiogenic capacity of RCC. These drugs were simulated in the treatment state by reducing the reaction rate of the activation of angiogenesis by both VEGF and

PDGF-β (Figure 8). This simulation caused a sharp decrease in angiogenesis in the treatment state.

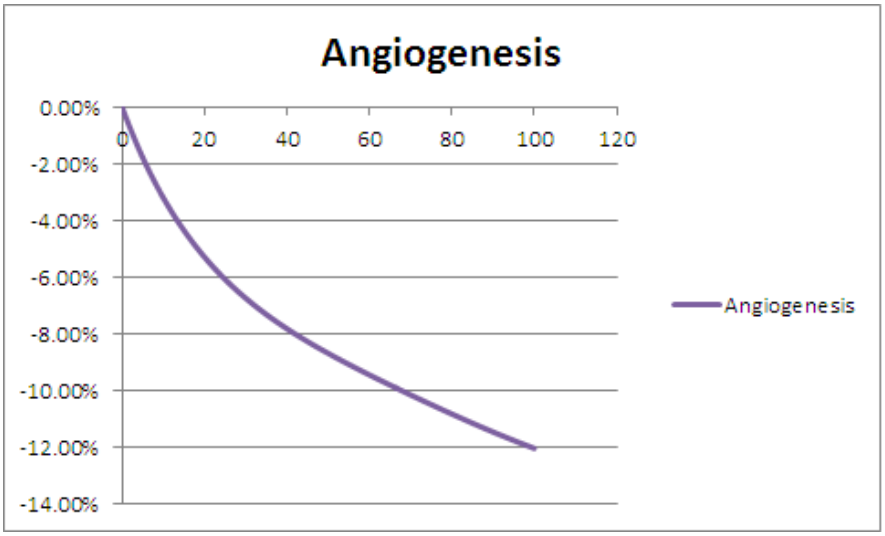

Figure 8. Effect of VEGF/PDGF inhibitor on angiogenesis.

3.2.2. mTORCI Inhibitor

The mTORCI inhibitor treatment state is based on the drug everolimus, which inhibit the kinase activity of mTORCI. This impairs the ability of mTORCI to activate the translation of HIF, which causes many downstream effects. These drugs were imitated by reducing reaction rate for the activation of mTORCI, which activates proteins involved in ribosome biogenesis and leads to the activation of HIF. This simulation resulted in an overall decrease in active mTORCI (Figure 9). The strange shape of the decrease can be explained by the large number of proteins involved in the activation of mTORCI. As the model simulates the cell over time, the concentrations of activators of mTORCI increase, so there is less decrease over time. Interestingly, there is no change in the model associated with HIF when mTORCI is inhibited.

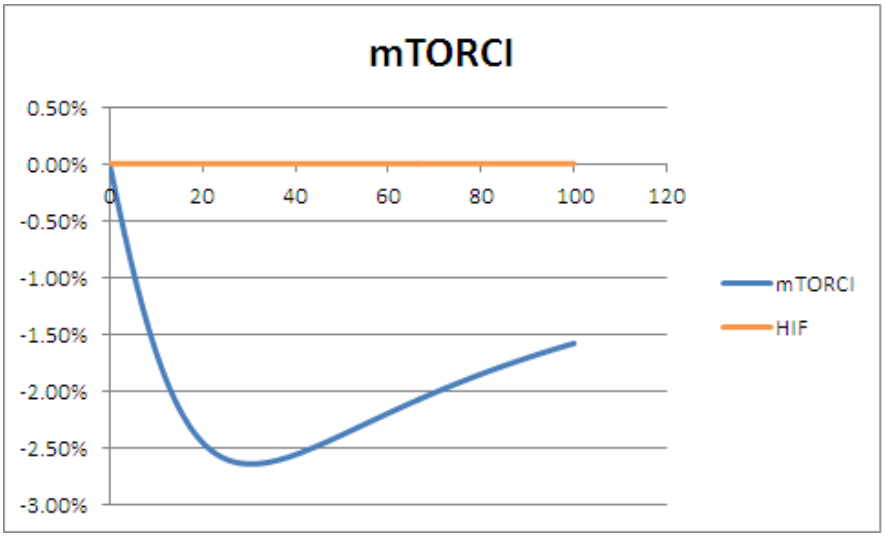

Figure 9. Efficacy of the mTORCI inhibitor.

The mTORCI inhibitor also causes lower concentrations of p53, MDM2, and NFκB (Figure 10). While there is no direct interaction between mTORCI and these transcription factors within the model, the slight decrease in these transcription factors could be due to a myriad of other changes.

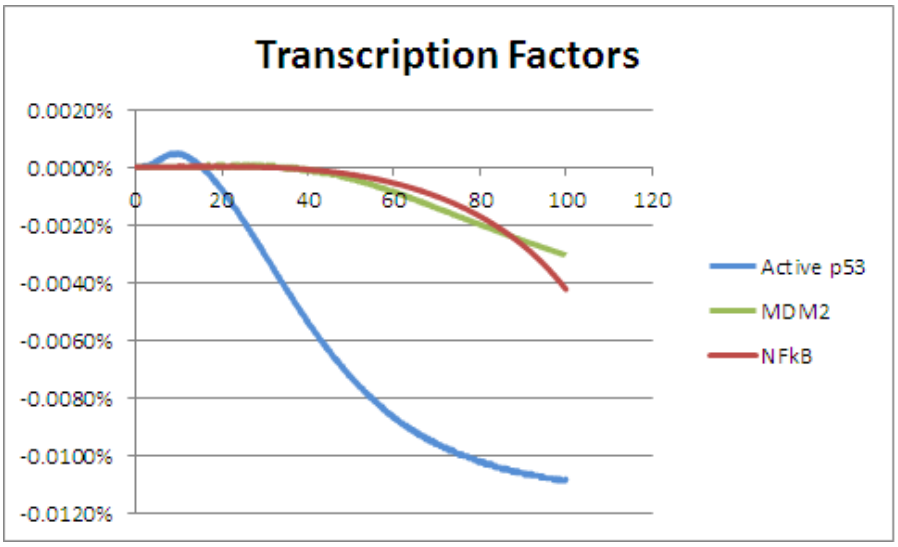

Figure 10. Effect of the mTORCI inhibitor on transcription factors.

Another effect of the mTORCI inhibitor is a slight decrease in the level of mitosis (Figure 11). This decrease could once again be due to a downstream change associated with cell cycle regulation.

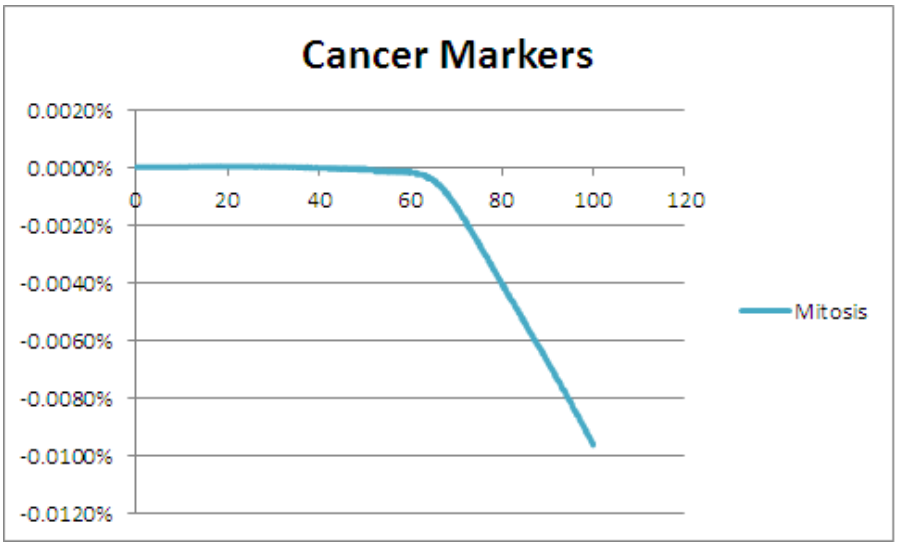

Figure 11. Effect of the mTORCI inhibitor on mitosis.

3.2.3. Cocktail Treatment

In order to test the efficacy of treating RCC with both an angiogenic inhibitor and a mTORCI inhibitor, a cocktail treatment was simulated in the model. This cocktail treatment was created by decreasing the reaction rates for the activation of angiogenesis via PDGF-β and VEGF and decreasing the reaction rate for mTORCI activation. The cocktail treatment showed combined effects from the individual treatments due to the fact that the treatments act on pathways that were modeled completely separately in the disease state. However, by combining the treatments a negative effect on both angiogenesis and mitosis can be observed, which could lead to a better prognosis than either treatment individually (Figure 12 and 13).

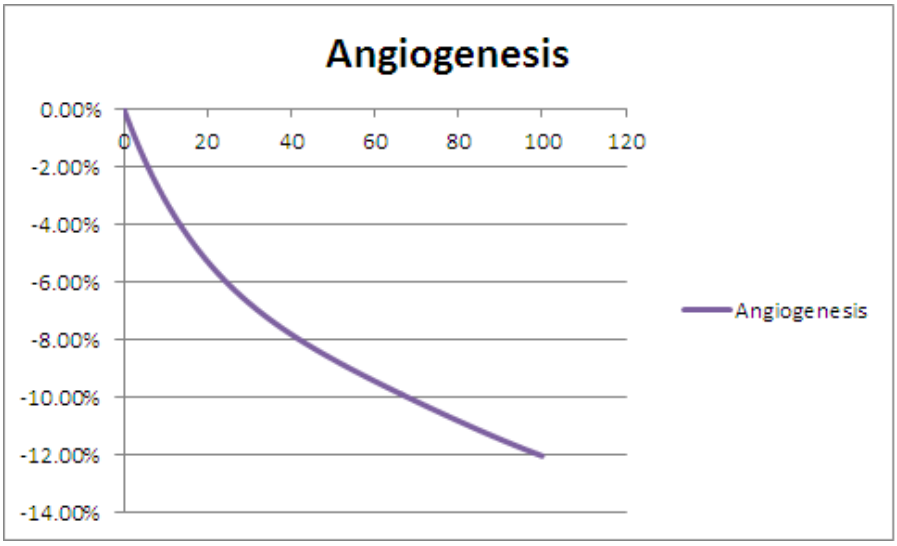

Figure 12. VEGF/PDGF inhibitor branch of the cocktail treatment.

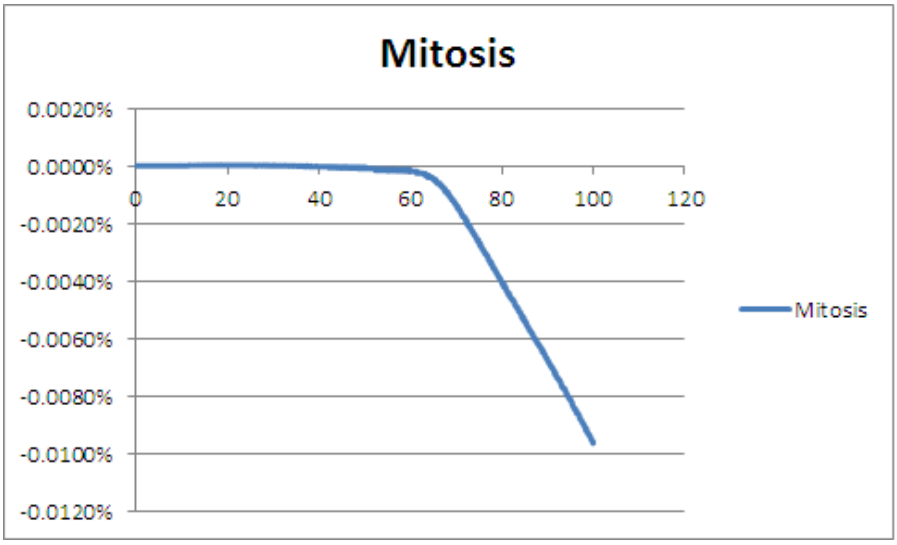

Figure 13. mTORCI inhibitor branch of the cocktail treatment.

4. Discussion

4.1. Disease State

The disease model when compared to the baseline model seems to accurately align with the experimental evidence observed in RCC. Figure 1 shows an decrease in pVHL and an increase in HIF. The inactivation of either one of both pVHL alleles is a phenomenon

often observed in ccRCC (Hervouet, 2007). In absence of a function pVHL protein, HIF-α is not degraded and instead combines with the constitutively expressed HIF-β to form transcription factor HIF. The increase in HIF contributes to the changes to glucose metabolism consistent with the Warburg effect observed in Figure 2. HIF upregulates the transcription of proteins involved in glycolysis such as Glut1, LDH, and PDK1 (Hamanaka, 2012). This causes increased levels of glycolysis and increased lactate production, but lower levels of oxidative phosphorylation. This holds true in the disease state until the end of the iteration where the levels of oxidative phosphorylation and acetyl coA production begin to catch up to the production of lactate; this unexpected observation is most likely due to the simplified way in which the TCA cycle and oxidative phosphorylation were modeled. The increase of ribose-5-phosphate is also consistent with the Warburg effect because an increased in glycolysis would lead to an increase in biosynthetic intermediates such as ribose-5-phosphate in the pentose phosphate pathway.

The increase in NFκB and Myc-Max observed in Figure 3 is also consistent with RCC. In a 2003 study by Oya et al., tissue NFκB expression was increased more than two-fold in 13 out of 45 samples of RCC; the majority of these 13 were metastatic tumors (Oya, 2003). Myc expression is also upregulated in RCC; according to a 2009 study by Tang et al. the average expression of Myc in ccRCC tissue samples is much higher than in normal kidney samples (Tang, 2009). The transcription factor p53 and its inhibitor MDM2 are also expressed at higher concentrations in RCC (Figure 4) (Noon, 2010). MDM2 and p53 are both associated with tumor progression and are both potential prognostic markers for

RCC. Upregulation of these proteins is detected is most but not all tissues samples of RCC.

Figure 5 and 6 relate to the effect of the disease state of RCC on the mTOR pathway. In a 2005 study, Hara et al. found that active AKT was significantly increased in RCC tissue as opposed to normal kidney tissue (Hara, 2005). mTORCI is also found to be upregulated in RCC tissue (Abraham, 2007).

A malignant cancer phenotype has several attributes: self-sufficient growth, resistance to apoptosis, and sustained angiogenesis (Morais, 2011). Therefore, in order to truly analyze the effect of the disease state of RCC, these factors must be analyzed. In Figure 7, apoptosis is decreasing while mitosis and angiogenesis are increasing. In the model apoptosis is decreasing as a result of several downstream anti-apoptotic signals such as the upregulation of glutaminase by Myc-Max and p53 in order to enhance the production of glutathione. Glutathione can prevent cellular damage from reactive oxygen species and stave off apoptosis (Cairns, 2011). Mitosis is increasing in the model due to many downstream signals such as the increased transcription of cyclins, CDKs, and activators of cyclins and CDKs (Lutz, 2002). The increase in angiogenesis in the model is due to the upregulation of PDGF-β and VEGF from HIF and NFκB (Brugarolas, 2009). Overall, this result matches a malignant phenotype and further solidifies the suitability of the disease state of RCC for treatment testing.

4.2. Treatment State

Due to a its central role in the pathway, there has been a high interest in disrupting the HIF pathway, either up or downstream (Patel, 2006). The treatments presented in this

paper deal with treating RCC through HIF through both an upstream and downstream mechanism. One strategy involves treating the downstream effectors of HIF in order to prevent their effect. The first treatment inhibits the activation of angiogenesis by inhibiting PDGF-β and VEGF. Sunitinib acts by inhibiting the VEGF and PDGF-β receptors by competitively binding with ATP at the tyrosine kinase active site. The treatment state utilizing sunitinib did reduce angiogenesis, but since angiogenesis is not a focus of the RCC disease state model, more results could not be gleaned (Figure 8). Another option for treating RCC is to treat an upstream activator of HIF. mTOR inhibitors fill this role by preventing the activation of mTORCI and thus preventing it from activating the translation of HIF. Everolimus is a serine/threonine kinase inhibitor that prevents the activation of the mTOR pathway. Treatment with everolimus did reduce levels of mTORCI, but it did not reduce levels of HIF (Figure 9). Because this consequence does not make sense biochemically, the lack of reduction in HIF may be a shortcoming of the mathematical model. Despite not effecting HIF, the everolimus treatment did decrease the amounts of p53, MDM2, and NFκB through unknown downstream effects (Figure 10); this change could explain some of the extended survival associated with everolimus treatment. Additionally, treatment with everolimus slightly decreased the amount of mitosis within the renal cell, which is a marker of a less virulent cancer (Figure 11).

In order to test the effect of combining multiple pathway treatments on RCC, a cocktail treatment of everolimus and sunitinib was generated mathematically. There were no effects from the treatments together that were not seen individually; however, combining the effects of the two treatments may lead to a better prognosis. In in a 2012 study by

Molina et al., a cocktail treatment of sunitinib and everolimus was tested in eligible patients (Molina, 2012). Unfortunately, the combination of these two drugs was associated with significant acute and chronic toxicities and had to be discontinued.

5. Conclusions and Future Directions

Renal cell carcinoma is a deadly form of cancer for which there is currently no effective treatment. Despite the strides made in cancer research, the mortality rate for RCC is still very high. Current research is focusing on inhibiting parts of the HIF pathway in order to slow the course of RCC. Two current treatments, growth factor inhibitors and mTOR inhibitors have shown promise individually, but together the treatments prove toxic. The RCC model suggests that the angiogenesis inhibitor, sunitinib, is successful in treating RCC by reducing angiogenesis. However, since angiogenesis was not modeled in-depth, the results are inconclusive. In the future, expanding the model to show more details of the angiogenesis pathway is recommended. The mTORCI inhibitor everolimus showed promise by reducing several markers of RCC, however, the treatment did not reduce levels of HIF. A reduction in HIF is to be expected in a RCC treatment that targets the mTOR pathway. In future works, the mTOR and HIF pathways should be reevaluated to make them more sensitive to treatment. Since the combination of these drugs produced toxicity in drug trials, a cocktail of the two is not recommended. Since the RCC model has been created, new treatments can be tested. In the future, treatments that affect other pathways in RCC may be tested, such as the c-myc, NFκB, or p53 pathways. Potentially, a drug that treated one of these pathways could improve other areas involved in RCC and

perhaps be coupled with sunitinib or everolimus to provide a more complex treatment. Hopefully one day a more specific chemotherapeutic or combination of chemotherapeutics can be created that will improve the prognosis of RCC.

Works Cited

Abraham, R.T., and Gibbons, J.J. (2007). The Mammalian Target of Rapamycin Signaling Pathway: Twists and Turns in the Road to Cancer Therapy. Clin Cancer Res *13*, 3109–3114.

Brugarolas, J. (2009). Molecular Pathways and Targeted Therapies for Renal Cell Carcinoma. *ASCO Educational Book, 2009*(1), 710.

Cairns, R.A., Harris, I.S., and Mak, T.W. (2011). Regulation of cancer cell metabolism. Nat Rev Cancer *11*, 85–95.

Hamanaka, R.B., and Chandel, N.S. (2012). Targeting glucose metabolism for cancer therapy. J Exp Med *209*, 211–215.

Hara, S., Oya, M., Mizuno, R., Horiguchi, A., Marumo, K., and Murai, M. (2005). Akt activation in renal cell carcinoma: contribution of a decreased PTEN expression and the induction of apoptosis by an Akt inhibitor. Ann Oncol *16*, 928–933.

Herman, J.G., Latif, F., Weng, Y., Lerman, M.I., Zbar, B., Liu, S., Samid, D., Duan, D.S., Gnarra, J.R., and Linehan, W.M. (1994). Silencing of the VHL tumor-suppressor gene by DNA methylation in renal carcinoma. Proc Natl Acad Sci U S A *91*, 9700–9704.

Hervouet, E., Simonnet, H., and Godinot, C. (2007). Mitochondria and reactive oxygen species in renal cancer. Biochimie *89*, 1080–1088.

Khan, A.A. (2010). Intracellular Mechanisms of Apoptosis. Journal of Biological Sciences *10*, 291–305.

Kitano, H., Funahashi, A., Matsuoka, Y., and Oda, K. (2005). Using process diagrams for the graphical representation of biological networks. Nat Biotech *23*, 961–966.

Larsson, L.-G., and Henriksson, M.A. (2010). The Yin and Yang functions of the Myc oncoprotein in cancer development and as targets for therapy. Experimental Cell Research *316*, 1429–1437.

Lutz, W., Leon, J., and Eilers, M. (2002). Contributions of Myc to tumorigenesis. Biochimica Et Biophysica Acta (BBA) - Reviews on Cancer *1602*, 61–71.

Mathupala, S.P., Ko, Y.H., and Pedersen, P.L. (print). Hexokinase II: Cancer's double-edged sword acting as both facilitator and gatekeeper of malignancy when bound to mitochondria. Oncogene *25*, 4777–4786.

Micheau, O., and Tschopp, J. (2003). Induction of TNF Receptor I-Mediated Apoptosis via Two Sequential Signaling Complexes. Cell *114*, 181–190.

Molina, A.M., Feldman, D.R., Voss, M.H., Ginsberg, M.S., Baum, M.S., Brocks, D.R., Fischer, P.M., Trinos, M.J., Patil, S., and Motzer, R.J. (2012). Phase 1 trial of everolimus plus sunitinib in patients with metastatic renal cell carcinoma. Cancer *118*, 1868–1876.

Morais, C., Gobe, G., Johnson, D.W., and Healy, H. (2011). The emerging role of nuclear factor kappa B in renal cell carcinoma. The International Journal of Biochemistry & Cell Biology *43*, 1537–1549.

Motzer, R.J., and Russo, P. (2000). Systemic therapy for renal cell carcinoma. J. Urol. *163*, 408–417.

Noon, A.P., Vlatković, N., Polański, R., Maguire, M., Shawki, H., Parsons, K., and Boyd, M.T. (2010). p53 and MDM2 in renal cell carcinoma. Cancer *116*, 780–790.

Oya, M., Takayanagi, A., Horiguchi, A., Mizuno, R., Ohtsubo, M., Marumo, K., Shimizu, N., and Murai, M. (2003). Increased nuclear factor-κB activation is

related to the tumor development of renal cell carcinoma. Carcinogenesis *24*, 377–384.

Patel, P.H., Chadalavada, R.S.V., Chaganti, R.S.K., and Motzer, R.J. (2006). Targeting von Hippel-Lindau Pathway in Renal Cell Carcinoma. Clin Cancer Res *12*, 7215–7220.

Rini, B.I., Campbell, S.C., and Escudier, B. (2009). Renal cell carcinoma. Lancet *373*, 1119–1132.

Sass, M.B., Lorenz, A.N., Green, R.L., and Coleman, R.A. (2009). A pragmatic approach to biochemical systems theory applied to an alpha-synuclein-based model of Parkinson's disease. J. Neurosci. Methods *178*, 366–377.

Savageau, M.A. (1969). Biochemical systems analysis. II. The steady-state solutions for an n-pool system using a power-law approximation. J. Theor. Biol. *25*, 370–379.

Vermeulen, K., Berneman, Z.N., and Van Bockstaele, D.R. (2003). Cell cycle and apoptosis. Cell Proliferation *36*, 165–175.

Voit, E.O. (2000). Computational Analysis of Biochemical Systems: A Practical Guide for Biochemists and Molecular Biologists (Cambridge University Press).

Additional Model Citations

Curthoys, N.P., and Watford, M. (1995). Regulation of glutaminase activity and glutamine metabolism. Annu. Rev. Nutr. 15, 133–159.

Matés, J.M., and Sánchez-Jiménez, F.M. (2000). Role of reactive oxygen species in apoptosis: implications for cancer therapy. Int. J. Biochem. Cell Biol. 32, 157–170.

Mckee, Trudy, and James McKee. Biochemistry: The Molecular Basis of Life. 4th edition. New York: Oxford University Press, 2009. Print.

Ozben, T. (2007). Oxidative stress and apoptosis: Impact on cancer therapy. Journal of Pharmaceutical Sciences 96, 2181–2196.